

Nucleon form factors and the pion-nucleon sigma term

Rajan Gupta,^{a,*} Tanmoy Bhattacharya,^a Vincenzo Cirigliano,^a Martin Hoferichter,^b Yong-Chull Jang,^c Balint Joo,^d Emanuele Mereghetti,^a Santanu Mondal,^{a,e} Sungwoo Park,^{a,g} Frank Winter^g and Boram Yoon^h

^a*Los Alamos National Laboratory, Theoretical Division T-2, Los Alamos, NM 87545, USA*

^b*Albert Einstein Center for Fundamental Physics, Institute for Theoretical Physics, University of Bern, Sidlerstrasse 5, 3012 Bern, Switzerland*

^c*Physics Department, Columbia University, New York, NY 10027, USA*

^d*Oak Ridge Leadership Computing Facility, Oak Ridge National Laboratory, Oak Ridge, TN 37831, USA*

^e*Department of Physics and Astronomy, Michigan State University, MI, 48824, USA*

^f*Department of Computational Mathematics, Science and Engineering, Michigan State University, MI, 48824, USA*

^g*Jefferson Lab, 12000 Jefferson Avenue, Newport News, Virginia 23606, USA*

^h*Los Alamos National Laboratory, Computer Computational and Statistical Sciences Division, CCS-7, Los Alamos, NM 87545, USA*

E-mail: rajan@lanl.gov

This talk summarizes the progress made since Lattice 2021 in understanding and controlling the contributions of towers of multihadron excited states with mass gaps starting lower than of radial excitations, and in increasing our confidence in the extraction of ground state nucleon matrix elements. The most clear evidence for multihadron excited state contributions (ESC) is in axial/pseudoscalar form factors that are required to satisfy the PCAC relation between them. The talk examines the broader question—*which and how many of the theoretically allowed positive parity states $N(\mathbf{p})\pi(-\mathbf{p})$, $N(\mathbf{0})\pi(\mathbf{0})\pi(\mathbf{0})$, $N(\mathbf{p})\pi(\mathbf{0})$, $N(\mathbf{0})\pi(\mathbf{p})$, ... make significant contributions to a given nucleon matrix element?* New data for the axial, electric and magnetic form factors are presented. They continue to show trends observed in Ref. [1]. The N²LO χ PT analysis of the ESC to the pion-nucleon sigma term, $\sigma_{\pi N}$, has been extended to include the Δ as an explicit degree of freedom [2]. The conclusion reached in Ref. [3] that $N\pi$ and $N\pi\pi$ states each contribute about 10 MeV to $\sigma_{\pi N}$, and the consistency between the lattice result with $N\pi$ state included and the phenomenological estimate is not changed by this improvement.

The 39th International Symposium on Lattice Field Theory (LATTICE2022) 8–13 August, 2022 Bonn, Germany

*Speaker

1. Introduction

The neutron and proton are stable bound states of quarks and gluons whose structure is governed by Quantum Chromodynamics. (In this talk, weak decays, isospin breaking and electromagnetic corrections are ignored.) Simulations of lattice QCD are being used to predict their properties with increasing control over all systematic uncertainties. In addition to controlling the three standard systematics: extrapolation to the continuum ($a \rightarrow 0$) and infinite volume ($L \rightarrow \infty$) limits and evaluating the results at $M_\pi = 135$ MeV, there are two additional interrelated challenges to precision calculations of nucleon properties. The first is the exponential fall-off of the signal to noise ratio proportional to $e^{-(M_N - 1.5M_\pi)\tau}$ in all nucleon correlation functions. In the state-of-the-art calculations with $O(10^6)$ measurements on about 5000 configurations, a good statistical signal extends up to ≈ 2 fm in 2-point correlation functions and up to ≈ 1.5 fm in 3-point functions (see Ref. [1] for background, notation, methodology and description of lattices used). The second challenge is that at these source-sink separations, ESC are significant even in the simplest observables such as nucleon charges (see Fig. 5), and in some channels (such as the matrix element of the fourth component of the axial current) they dominate the signal [1, 4].

Theoretically, we know how to extract the matrix elements (ME) of various operators within the ground state nucleon. These are obtained by making fits to the spectral decompositions of the correlation functions that are the ensemble averages of quark-line diagrams shown in Fig. 1. The spectral decomposition of the 2- and 3-point correlation functions with the insertion of the current $\hat{J}_\mu (= \hat{A}_\mu, \hat{V}_\mu, \hat{P}, \hat{S}, \hat{T}_{\mu\nu})$ at time t and with source-sink separation τ are given by

$$\Gamma_N^2 = \sum_i |\langle \Omega | \hat{N} | N_i \rangle|^2 e^{-E_i \tau}; \quad \Gamma_N^3 = \sum_{i,j} \langle \Omega | \hat{N} | N_i \rangle^* e^{-E_i(\tau-t)} \langle N_i | \hat{J}_\mu | N_j \rangle e^{-E_j t} \langle N_j | \hat{N} | \Omega \rangle, \quad (1)$$

from which we extract $\langle N_0 | \hat{A}_\mu | N_0 \rangle$ and $\langle N_0 | \hat{V}_\mu | N_0 \rangle$ to calculate form factors. The most direct strategy to get these ME is to fit Γ_N^3 and resolve all the parameters. Even for a 2-state truncation of Eq. (1), this requires, in addition to $\langle N_0 | \hat{A}_\mu | N_0 \rangle$, resolving two energies, $E_{0,1}$, the amplitude $A_0 \equiv \langle \Omega | \hat{N}_i | N \rangle$, and the not subsequently used combinations: $A_0^* A_1 \langle N_0 | \hat{A}_\mu | N_1 \rangle$, $A_1^* A_0 \langle N_1 | \hat{A}_\mu | N_0 \rangle$ and $A_1^* A_1 \langle N_1 | \hat{A}_\mu | N_1 \rangle$. Unfortunately, totally unconstrained fits to current data at multiple values of $\{t, \tau\}$ are not sufficient to yield a unique solution (large regions of parameter space give roughly the same χ^2/dof), so the resulting uncertainty in $\langle N_0 | \hat{A}_\mu | N_0 \rangle$ can be large.

In principle, all states of the transfer matrix with quantum numbers of \hat{N} contribute to the sums in Eq. (1). This set of states are the same for Γ_N^2 and Γ_N^3 . Thus, if we could take all the E_i and A_0 from Γ^2 , fits to Γ^3 would be greatly improved and yield much better estimates for $\langle N_0 | \hat{A}_\mu | N_0 \rangle$. The challenge/question is—is the ordering of the states by the size of their contribution to Γ^2 the same as to Γ^3 ? The answer in many cases is NO. For many Γ^3 , contribution of towers of multihadron states, for example, $N(\mathbf{q})\pi(-\mathbf{q}), \forall \mathbf{q} \neq 0$ on the $\mathbf{p}_j = 0$ side in Γ^3 and $N(\mathbf{q})\pi(-(\mathbf{p} + \mathbf{q}))$ or $N(-(\mathbf{p} + \mathbf{q})\pi(\mathbf{q}), \forall \mathbf{q}$ on the $\mathbf{p}_i \neq 0$ side with $\mathbf{q} = \mathbf{p}_j - \mathbf{p}_i$ contribute in addition to single-particle excited states. Such towers of states, labeled by relative momenta \mathbf{q} , are typically not resolved in Γ^2 if a single nucleon interpolating operator such as $\hat{N}(x) = \epsilon^{abc} \left[q_1^{aT}(x) C \gamma_5 \frac{(1 \pm \gamma_4)}{2} q_2^b(x) \right] q_1^c(x)$ is used.

There are at least 5 states with positive parity and energy below $N(1440)$ for our ensembles: $N, N(0, 0, 1)\pi(0, 0, -1), N(0, 1, 1)\pi(0, -1, -1), N(0)\pi(0)\pi(0)$, and $N(0)\pi(1)\pi(-1)$. This number

grows as $\vec{q} \rightarrow 0$. To enlarge the number of states included in the fit (order of truncation in Eq. (1)) and yet nail the parameter space, one needs information from Γ^2 (at least E_0 and A_0) and physics inspired priors with narrow width for the E_i . On the output side, operationally, an n-state fit function incorporates the influence of all states that give significant contributions, so result of the fit for energies E_1 to E_{n-1} are some combinations of the energies of all the excited states of the transfer matrix.

This by itself is not a problem since we know approximately the energy of the radial excitations ($N^{1/2}(1440)$, $N^{1/2}(1710)$, ...) and of the non-interacting multihadron states, provided n-state fits with different selections of these states are distinguished by the χ^2/dof (i.e., a data driven analysis). For example, if the χ^2/dof of a 2-state fit with say $E_1 = E_{N(1440)}$ is significantly better than that with the lowest multihadron state with positive parity ($E_1 = E_N(0, 0, 1) + E_\pi(0, 0, -1) \sim 1230$ MeV), then picking the result with $E_{N(1440)}$ is justified. The problem we face is that the χ^2/dof of the fits to current data are similar whereas the values of $\langle N_0 | \hat{A}_\mu | N_0 \rangle$ obtained are significantly different. So one needs additional information to pick between fits with different excited states included. Here I describe two calculations for which ESC is significant and additional information is needed to decide between the fits. In the calculation of axial vector form factors it is satisfying the axial Ward identity, i.e., PCAC, and in the calculation of the pion-nucleon sigma term it is a χPT analysis.

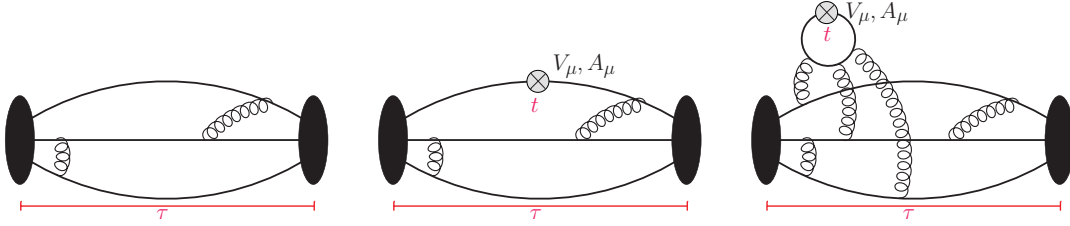


Figure 1: Illustration of quark-line diagrams for 2-point (left), connected 3-point with the insertion of vector and axial operators $\bar{u}\gamma_\mu d$ and $\bar{u}\gamma_5\gamma_\mu d$ (middle), and the additional disconnected contributions to matrix elements of flavor diagonal axial and vector operators $\bar{q}\gamma_\mu q$ and $\bar{q}\gamma_5\gamma_\mu q$ (right). The operator, axial/vector current, is inserted at intermediate Euclidean time t and with momentum \vec{q} . Each quark line represents the Feynman propagator, $S_F = \mathcal{D}^{-1}$, given by the inverse of the Dirac matrix on that configuration. From these correlation functions, we extract the axial/vector form factors of the nucleon as outlined in Sec. 3.

2. A tempered surprise in the spectrum from the nucleon 2-point function

The spectrum of the transfer matrix in a finite box with nucleon quantum numbers and lattice momenta $\mathbf{p} = \mathbf{n}2\pi/La$ can be determined from fits to the spectral decomposition of the two-point function Γ^2 given in Eq. (1). But how well do fits to Γ^2 with an interpolating operator \hat{N} , which we tune to have minimum overlap with excited states, capture the states that are significant for Γ^3 ?

An example of the conundrum of ESC with a single nucleon operator is shown in Fig. 2 (left 2 panels) of fits to Eq. (1) truncated at four states using high statistics $a091m170$ data. (See Ref. [1] for details.) The left panel shows the standard analysis with wide priors used only to stabilize the fit, while the second panel shows a fit with a narrow prior for E_1 taken to be the energy of a non-interacting $N(\mathbf{1})\pi(-\mathbf{1})$ state. The resulting E_1 are about 1.5 and 1.2 GeV, respectively. The two outcomes are not distinguished by the augmented χ^2 minimized in the fits. In fact, in these 4-state fits there is a whole region of parameter space that gives similar χ^2 in which E_1 between 1.2 – 1.5 GeV

is equally likely. Furthermore, assuming $R_1 \equiv |\mathcal{A}_1/\mathcal{A}_0|^2 \approx 1$, the contribution of a state with $\Delta E_1 = 300$ MeV is still 20% (5%) at $\tau/a = 11$ (22), i.e., at source-sink separation τ of 1 fm (2fm).

New data on the $a071m170$ and $a070m130$ ensembles break from the above pattern seen on the other 11 ensembles. Here, the “standard” $\{4\}$ and the $\{4^N\pi\}$ fits give very similar spectrum (E_i and A_i) with $E_1 \approx E_{N\pi}$ and a large $E_2 > 2$ GeV (panels 3 and 4 in Fig. 2 for $a070m130$). The eventuality that different initial points (priors) lead to the same minimum and expose the $N\pi$ state in Γ^2 as $M_\pi \rightarrow 135$ MeV and $a \rightarrow 0$ is very encouraging. Unfortunately, the $a070m130$ result is not stable, but has depended on the statistics, leaving open the question—what statistics will be needed to expose the multihadron states in Γ^2 ? Our current effort is to include 2 excited states to analyze Γ^3 by trying different combinations of possible states and input their E_1 and E_2 with physics driven narrow priors.

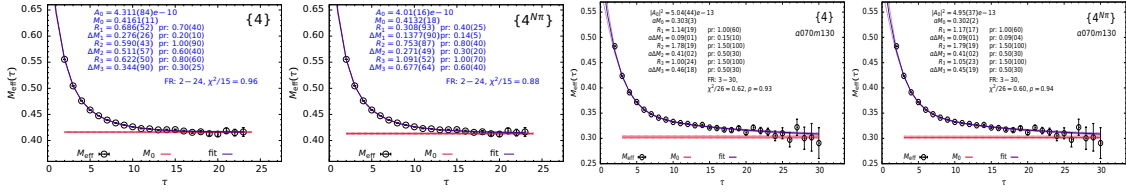


Figure 2: Nucleon effective mass plots. The “standard” $\{4\}$ and the $\{4^N\pi\}$ fits to $a091m170$ ensemble data (left two panels) give different estimates of E_i and A_i . Fits to the $a070m130$ data give consistent estimates.

3. Extraction of form factors

The Lorentz covariant decomposition of the iso-vector matrix elements (ME) calculated within the nucleon ground state $|N(\mathbf{p}_i, s_i)\rangle$ extracted from the 3-point functions with the insertion of the renormalized isovector axial, $A_\mu = Z_A \bar{u} \gamma_5 \gamma_\mu d$ and pseudoscalar $P = Z_P \bar{u} \gamma_5 d$ currents with momentum transfer $\vec{q} = \vec{p}_f - \vec{p}_i$ gives, in Euclidean space, the axial, $G_A(Q^2)$, induced pseudoscalar, $\tilde{G}_P(Q^2)$, and the pseudoscalar, $G_P(Q^2)$, form factors:

$$\begin{aligned} \langle N(\mathbf{p}_f, s_f) | A_\mu(\mathbf{q}) | N(\mathbf{p}_i, s_i) \rangle &= \bar{u}_N(\mathbf{p}_f, s_f) \left(G_A(Q^2) \gamma_\mu + q_\mu \frac{\tilde{G}_P(Q^2)}{2M_N} \right) \gamma_5 u_N(\mathbf{p}_i, s_i), \\ \langle N(\mathbf{p}_f) | P(\mathbf{q}) | N(\mathbf{p}_i) \rangle &= \bar{u}_N(\mathbf{p}_f) G_P(Q^2) \gamma_5 u_N(\mathbf{p}_i), \end{aligned} \quad (2)$$

where $Q^2 \equiv \mathbf{p}^2 - (E_f - E_i)^2 = -q^2$ is the spacelike four-momentum squared. These three form factors must satisfy, up to discretization errors, the following relation

$$2\hat{m}G_P(Q^2) = 2M_N G_A(Q^2) - \frac{Q^2}{2M_N} \tilde{G}_P(Q^2), \quad (3)$$

that follows from the axial Ward identity, $\partial_\mu Z_A A_\mu - 2Z_m m Z_P P = 0$. Here $\hat{m} \equiv Z_m Z_P (m_u + m_d)/(2Z_A)$ is the average bare PCAC mass of the u and d quarks. Result of this test for the 2-state strategy $\{4^N\pi, 2^{\text{sim}}\}$ [1], shown in the top row of Fig. 3, indicates a growing deviation as $Q^2 \rightarrow 0$, especially in the physical pion mass ensemble $a070m130$. This suggests the need for a tuned E_2 .

Similarly, insertion of $V_\mu = Z_V \bar{u} \gamma_\mu d$, gives the Dirac $F_1(q^2)$ and Pauli $F_2(q^2)$ form factors:

$$\langle N(\mathbf{p}_f, s_f) | V_\mu^{\text{em}}(\mathbf{q}) | N(\mathbf{p}_i, s_i) \rangle = \bar{u}_N(\mathbf{p}_f, s_f) \left(F_1(Q^2) \gamma_\mu + \sigma_{\mu\nu} q_\nu \frac{F_2(Q^2)}{2M_N} \right) u_N(\mathbf{p}_i, s_i), \quad (4)$$

in terms of which the electric, G_E , and magnetic, G_M , form factors are given by

$$G_E(Q^2) = F_1(Q^2) - \frac{Q^2}{4M_N^2} F_2(Q^2), \quad (5)$$

$$G_M(Q^2) = F_1(Q^2) + F_2(Q^2). \quad (6)$$

In addition to the PCAC constraint in Eq. (3), these form factors have 4 experimental constraints: the conserved vector charge $g_V = G_E|_{Q^2=0} = F_1|_{Q^2=0} = 1$, the difference of magnetic moments $(\mu^P - \mu^N) = G_M|_{Q^2=0} = (F_1 + F_2)|_{Q^2=0} = 4.7059$, the axial charge $g_A = G_A|_{Q^2=0} = 1.276(2)$ from neutron β -decay, and $\tilde{G}_P|_{(Q^2=0.88m_\mu^2)} = 8.06(55)$ from muon capture in the MuCap experiment [5]. The goal is to determine the Q^2 behavior of these 5 form factors using lattice QCD with control over all sources of errors.

4. Progress in the calculation of form factors since Lattice 2021

Our latest published results for the axial and vector form factors in Ref. [1] are based on seven 2+1-flavor Wilson-clover ensembles, and these data were discussed at lattice 2021. Two of these seven ensembles provided a finite volume study, thus the data were at five distinct values of $\{a, M_\pi\}$. This calculation has been extended to 13 ensembles with 11 distinct values of $\{a, M_\pi\}$ with $M_\pi L > 4$. These data, especially the physical pion mass ensemble $a070m130$ (only 40% analyzed), should be considered preliminary. A summary of the highlights is

- **Axial form factor:** In Ref. [6], we first pointed out that the axial form factors obtained using the “standard” method with excited state energies E_i taken from Γ^2 fail to satisfy the PCAC relation. The reason for this failure was identified in Ref. [4], and fits to the data for the 3-point function $\langle \Omega | \hat{N}^\dagger A_4 \hat{N} | \Omega \rangle$ confirmed the χPT analysis [7] that the $N\pi$ excited state contribution to the ME is enhanced and very significant. Two analysis strategies were developed to include the $N\pi$ state in accord with the pion-pole dominance hypothesis. In the first labeled $\{4^{N\pi}, 3^*\}$, we input via a narrow prior the non-interacting energy of the $N(0,0,1)\pi(0,0,-1)$ state for E_1 in a 4-state fit to Γ^2 and use the output E_i in a 3-state fit to Γ^3 . In the second labeled $\{4^{N\pi}, 2^{\text{sim}}\}$, we make a simultaneous fit to the five correlation functions with insertions of A_μ and P and take only E_0 and A_0 from Γ^2 . In $\{4^{N\pi}, 2^{\text{sim}}\}$, the data for A_4 (which are dominated by the excited state) drive the determination of E_1 that ends up being close to $N(0,0,1)\pi(0,0,-1)$, especially as $M_\pi \rightarrow 135$ MeV. The advantage of the second method is—it is totally data driven but the disadvantage is it is, so far, only 2-state (adding a third state brings in priors). The comparison of the new and old results with $\{4^{N\pi}, 2^{\text{sim}}\}$ is presented in the second row of Fig. 3. The enlarged data set continues to show mild dependence on a and M_π .
- **PCAC:** Data in first row of Fig. 3 show a significant ($\sim 12\%$) drop in the $a070m130$ data as $Q^2 \rightarrow 0$ compared to $\approx 50\%$ without $N\pi$ in the analysis [6]. We are investigating whether this indicates the need for a second low mass excited state added to the $\{4^{N\pi}, 2^{\text{sim}}\}$ analysis.
- **Electric and magnetic form factors:** the data (except for the preliminary $a070m130$ data) in rows 3-4 of Fig. 3 continue to show little dependence on a and M_π and agree with the Kelly

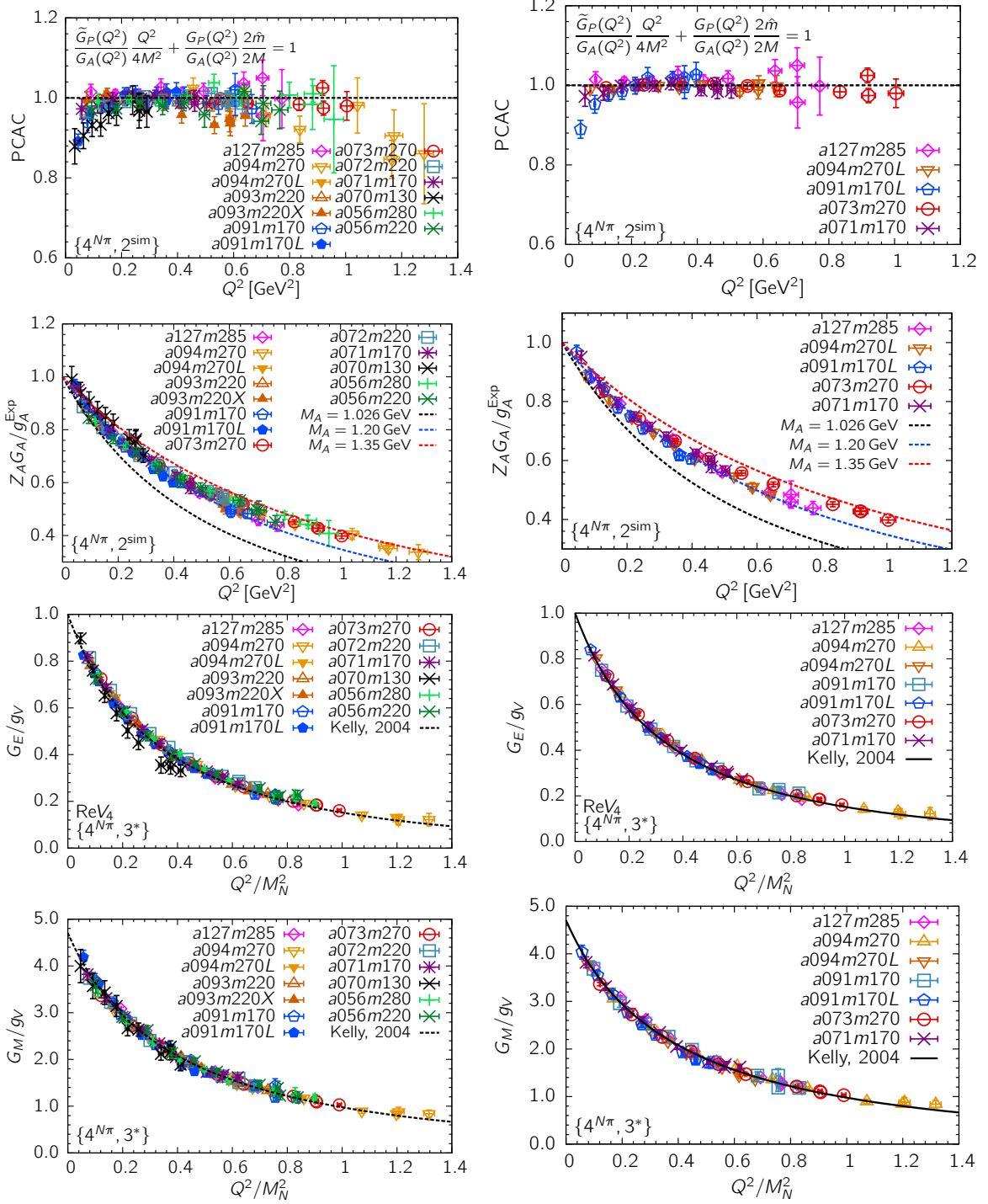


Figure 3: Comparison of the preliminary data from 13 ensembles (left) with that published in Ref. [1] from 7 ensembles (right). The top row shows the degree to which the axial form factors satisfy the PCAC relation, Eq. (3). Rows 2-4 compare the axial $G_A(Q^2)$, the electric $G_E(Q^2)$, and the magnetic $G_M(Q^2)$ form factors. The statistics on the new $M_\pi \approx 130$ MeV ensemble $a070m130$ are 40% of the target 2500 lattices.

parameterization of the experimental data. Our best fit is $\{4^{N\pi}, 3^*\}$ which includes a prior for E_1 that is close to the $N\pi\pi$ state (on our lattices $E(N(0)\pi(0)\pi(0)) \approx E(N(1)\pi(-1))$). The sensitivity of results to the value of E_1 is, however, much smaller than in the axial case. This is not unreasonable since vector meson dominance suggests a coupling to the ρ -meson (a $\pi\pi$ state), however, since it is much heavier than the pion, the effect is likely to be smaller. Chiral PT analysis by Bär in Ref. [8] indicates a $\approx 5\%$ effect due to the pion loop. The Q^2 dependence and the magnitude of the effect is consistent with the pattern seen in a summary of world lattice data with the “standard” method shown in fig. [22] in Ref. [9]. If the favorable situation shown here (EM form factors have small systematics) persists, then increasing the statistics and adding more ensembles is a viable strategy for precision results in the near future.

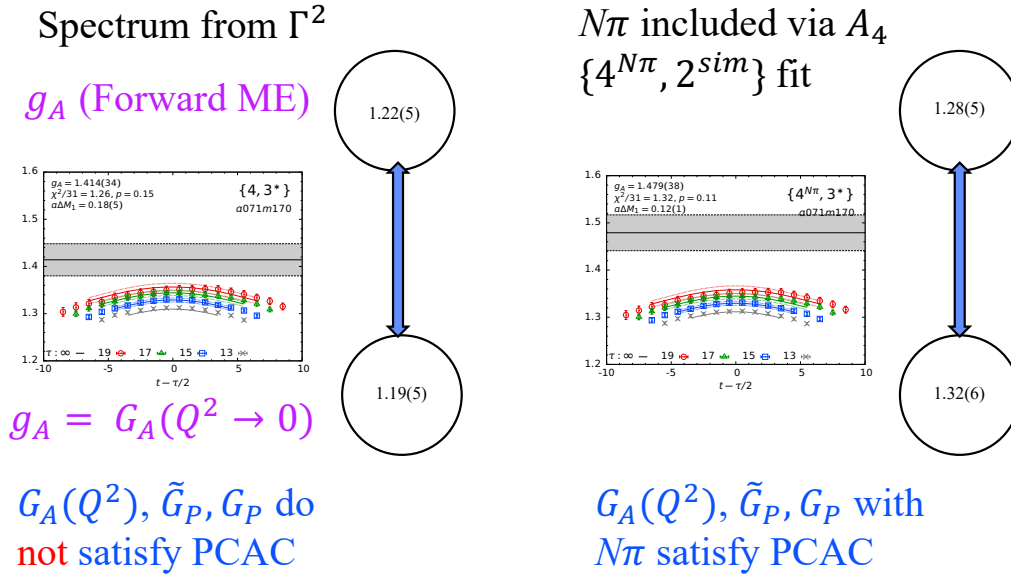


Figure 4: Comparison of two strategies for extracting g_A^{u-d} : (left) using the standard method, and (right) including $N(0, 0, 1)\pi(0, 0, -1)$ state in the analysis of both the forward matrix element and of the form factors.

5. Analysis of the isovector axial charge g_A^{u-d}

The issue of which excited states need to be included in the analysis of the charge g_A^{u-d} is subtle (see [10] for background). The enhanced effect of the $N(0, 0, 1)\pi(0, 0, -1)$ state to the ME in the form factors analysis, vanishes as $\vec{q} \rightarrow 0$, however, this state still contributes at 1-loop in χPT and could be a $\sim 5\%$ effect. In Fig. 4 we illustrate a consistency check that indicates that the analysis including the $N(0, 0, 1)\pi(0, 0, -1)$ state is required. The figure illustrates a comparison of two strategies for extracting g_A^{u-d} with all the numbers taken from Ref. [1]. On the left hand side is the “standard” analysis of g_A^{u-d} extracted both from the forward matrix element and from $G_A(Q^2 \rightarrow 0)$. These two estimates must agree by continuity! They do but the value is $\approx 5\%$ smaller than experiment. Most important—the form factors **do not** satisfy PCAC. The right part shows the $\{4^{N\pi}, 2^{sim}\}$ analysis with $E_1 \approx E(N(0, 0, 1)\pi(0, 0, -1))$. Again the two values agree, are about 6% larger than the “standard” value, still consistent with experiment, and **the form factors satisfy PCAC**. Final analysis of all 13 ensembles, keeping in mind the discussion in Sec. 2, is underway!

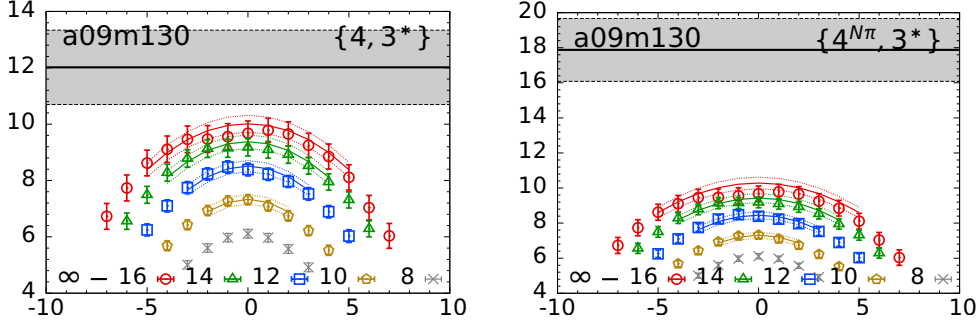


Figure 5: The data for g_S^{u+d+2l} from the physical mass, $a09m130$ ensemble and the two fits to remove ESC. (Left) standard analysis and (Right) including $N\pi$ and $N\pi\pi$ states. Both panels are reproduced from [3].

6. The pion-nucleon sigma term

Flavor diagonal scalar charges of the nucleon, $g_S^{u,d,s,c}$, are important for many analyses such as the spin independent cross-section of dark matter with nuclear targets [11, 12], lepton flavor violation in $\mu \rightarrow e$ conversion in nuclei [13, 14], and in electric dipole moments [15, 16]. These are obtained from the forward matrix element of the scalar density $\bar{q}q$ (here it is implicit that the subtracted operator, $\bar{q}q - \langle \Omega | \bar{q}q | \Omega \rangle$), is used as discussed in Ref. [17]) between the nucleon ground state:

$$g_S^q = \langle N(\mathbf{k} = 0, s) | \bar{q}q | N(\mathbf{k} = 0, s) \rangle. \quad (7)$$

The pion–nucleon σ -term $\sigma_{\pi N} \equiv m_{ud} g_S^{u+d} \equiv m_{ud} \langle N(\mathbf{k}, s) | \bar{u}u + \bar{d}d | N(\mathbf{k}, s) \rangle$ is a fundamental parameter of QCD—it quantifies the amount of the nucleon mass that comes from u - and d -quark masses being non-zero. In addition to lattice calculations, $\sigma_{\pi N}$ has also been extracted phenomenologically from $\pi - N$ scattering via the Cheng–Dashen low-energy theorem [18, 19].

The FLAG 2021 report [10] highlights a tension between the lattice estimates that favor $\sigma_{\pi N} \approx 40$ MeV versus a value around $\sigma_{\pi N} \approx 60$ MeV from phenomenology [20, 21].

The N²LO χ PT analysis [3] shows that there is an enhanced contribution from $N\pi$ and $N\pi\pi$ states due to the large coupling of the scalar source to two pions, i.e., a large quark condensate [3], and a large disconnected contribution. Including the Δ as an explicit state in the χ PT analysis [2] does not change the conclusion in [3]. Our calculation, done in the isospin symmetric limit with $m_{ud} = (m_u + m_d)/2$, gives $\sigma_{\pi N} \approx 40$ MeV with the standard analysis (consistent with previous lattice estimates) while the χ PT motivated one, i.e., including contributions of $N\pi$ and $N\pi\pi$ states, gives $\sigma_{\pi N} \approx 60$ MeV, which is consistent with phenomenology. Our lattice analysis is very highly weighted by the data on the one physical M_π ensemble shown in Fig. 5. This is expected as the difference in the E_1 used in the two fits to remove ESC grows as $M_\pi \rightarrow 135$ MeV. Again, the two fits give different results but are not differentiated by the χ^2 . To reach discrimination, our estimate is a $\geq 10X$ increase in statistics to get similar precision at $\tau = 18, 20$ as on the current $\tau = 14, 16$ data. It is very important to confirm this exciting result on other physical pion mass ensembles.

7. Conclusions

While the lattice methodology for the extraction of matrix elements from correlation functions using spectral decomposition is robust and steady progress is being made in calculations, two related issues of the exponential decay of the statistical signal with source-sink separation in all nucleon n -point functions, and the contribution of low-lying multihadron excited states have to be addressed before claiming robust, high precision results. We have summarized our progress in the last year in the extraction of axial and electromagnetic form factors and in the pion-nucleon sigma term. Analyses with the inclusion of the " $N\pi$ " state changes the results very significantly in both cases, and we provide evidence that they should be included. Motivated by the deviation seen in the PCAC relation in Fig. 3, our current efforts are to determine which second excited state, gives the next largest contribution and to include it in the fits to further improve estimates of ground state matrix elements.

We conclude by mentioning related promising efforts to overcome the signal to noise problem by analytic continuation of the contour of integration (see Refs. [22, 23]), and for ESC, the use of a variational basis of nucleon interpolating operators that includes multihadron operators to project on to the ground state of the nucleon at much shorter source-sink separations [24].

Acknowledgments

The calculations presented are based on two sets of ensembles: the 2 + 1 + 1-flavor HISQ ensembles generated by the MILC collaboration and the 2 + 1-flavor Wilson-clover ensembles generated by the JLAB/W&M/LANL/MIT collaborations. The calculations used the Chroma software suite [25]. We gratefully acknowledge computing resources provided by NERSC; OLCF at Oak Ridge through ALCC awards NPH110 and LGT107, and INCITE awards PHY138 and HEP133; USQCD clusters; and LANL Institutional Computing. Support for this work was provided by the U.S. DOE Office of Science HEP and NP, and the SNSF. T. Bhattacharya and R. Gupta were partly supported by the U.S. DOE, Office of Science, HEP under Contract No. DE-AC52-06NA25396. T. Bhattacharya, R. Gupta, S. Mondal, S. Park, and B. Yoon were partly supported by the LANL LDRD program, and S. Park by the Center for Nonlinear Studies.

References

- [1] S. Park, R. Gupta, B. Yoon, S. Mondal, T. Bhattacharya, Y.-C. Jang et al., [2103.05599](#).
- [2] R. Gupta, T. Bhattacharya, M. Hoferichter, E. Mereghetti, S. Park and B. Yoon, in *10th International workshop on Chiral Dynamics*, 3, 2022, [2203.13862](#).
- [3] R. Gupta, S. Park, M. Hoferichter, E. Mereghetti, B. Yoon and T. Bhattacharya, *Phys. Rev. Lett.* **127** (2021) 242002 [[2105.12095](#)].
- [4] Y.-C. Jang, R. Gupta, B. Yoon and T. Bhattacharya, *Phys. Rev. Lett.* **124** (2020) 072002 [[1905.06470](#)].
- [5] MuCAP collaboration, V. A. Andreev et al., *Phys. Rev. C* **91** (2015) 055502 [[1502.00913](#)].
- [6] R. Gupta, Y.-C. Jang, H.-W. Lin, B. Yoon and T. Bhattacharya, *Phys. Rev. D* **96** (2017) 114503 [[1705.06834](#)].
- [7] O. Bär, *Phys. Rev. D* **99** (2019) 054506 [[1812.09191](#)].

- [8] O. Bär and H. Čolić, *Phys. Rev. D* **103** (2021) 114514 [2104.00329].
- [9] Y.-C. Jang, R. Gupta, H.-W. Lin, B. Yoon and T. Bhattacharya, *Phys. Rev. D* **101** (2020) 014507 [1906.07217].
- [10] FLAVOUR LATTICE AVERAGING GROUP (FLAG) collaboration, Y. Aoki et al., *Eur. Phys. J. C* **82** (2022) 869 [2111.09849].
- [11] A. Bottino, F. Donato, N. Fornengo and S. Scopel, *Astropart. Phys.* **18** (2002) 205 [hep-ph/0111229].
- [12] M. Hoferichter, P. Klos, J. Menéndez and A. Schwenk, *Phys. Rev. Lett.* **119** (2017) 181803 [1708.02245].
- [13] V. Cirigliano, R. Kitano, Y. Okada and P. Tuzon, *Phys. Rev. D* **80** (2009) 013002 [0904.0957].
- [14] A. Crivellin, M. Hoferichter and M. Procura, *Phys. Rev. D* **89** (2014) 093024 [1404.7134].
- [15] J. Engel, M. J. Ramsey-Musolf and U. van Kolck, *Prog. Part. Nucl. Phys.* **71** (2013) 21.
- [16] J. de Vries, E. Mereghetti, C.-Y. Seng and A. Walker-Loud, *Phys. Lett. B* **766** (2017) 254 [1612.01567].
- [17] T. Bhattacharya, R. Gupta, W. Lee, S. R. Sharpe and J. M. S. Wu, *Phys. Rev.* **D73** (2006) 034504 [hep-lat/0511014].
- [18] T. P. Cheng and R. F. Dashen, *Phys. Rev. Lett.* **26** (1971) 594.
- [19] L. S. Brown, W. J. Pardee and R. D. Peccei, *Phys. Rev. D* **4** (1971) 2801.
- [20] M. Hoferichter, J. Ruiz de Elvira, B. Kubis and Ulf-G. Meißner, *Phys. Rev. Lett.* **115** (2015) 092301 [1506.04142].
- [21] J. Ruiz de Elvira, M. Hoferichter, B. Kubis and Ulf-G. Meißner, *J. Phys. G* **45** (2018) 024001 [1706.01465].
- [22] M. L. Wagman and M. J. Savage, *Phys. Rev. D* **96** (2017) 114508 [1611.07643].
- [23] W. Detmold, G. Kanwar, H. Lamm, M. L. Wagman and N. C. Warrington, *Phys. Rev. D* **103** (2021) 094517 [2101.12668].
- [24] L. Barca, G. Bali and S. Collins, 2211.12278.
- [25] SciDAC, LHPC, UKQCD collaboration, R. G. Edwards and B. Joó, *Nucl. Phys. Proc. Suppl.* **140** (2005) 832 [hep-lat/0409003].